STUDY ON THE MORPHOLOGICAL AND OPTICAL PROPERTIES OF POROUS ANODIC ALUMINA

By

CHIN ING KHANG

Thesis submitted in fulfillment of the requirements
for the degree of
Master of Science

February 2016

ACKNOWLEDGEMENTS

First and foremost, I would like to express my gratitude to my supervisor, Dr. Yam Fong Kwong for his guidance and support throughout the project. Without his motivation and advice, this dissertation would not be possible to complete smoothly.

I would also like to thank my research colleagues from the group: Dr. Beh Khi Poay, Chai Yingqi, Ng Siow Woon, Tan Lay Kim, Cheong Yuit Ling and Mah Chai Fong who willing to share their knowledge to assist me complete my research. With this opportunity, I offer my sincerest thanks to Mr. Chai who gave me a hand when I was at a loss during the project. I am very grateful to him for his selflessness and always ready to help.

My appreciation goes to the staff of Nano-Optoelectronics Research and Technology Laboratory (N.O.R Lab) for their technical assistance during my laboratory work.

Last but not least, I owe my family and girlfriend a big thank for their patience, support and understanding throughout my study. Their urge also motivates me to complete my study on time.

TABLE OF CONTENTS

LIST OF TABLES

LIST OF FIGURES

LIST OF SYMBOLS

A	Area of circle
D_{int}	Interpore distance
D_p	Pore diameter
d	Diameter of circle
I	Maximum intensity
n	Number of pores
P	Porosity
R	Regularity ratio
S	Surface area
U	Anodizing voltage
$W_{1/2}$	Full width half-maximum
λ_i	Proportional constant

LIST OF ABBREVIATIONS

1D	One-dimensional
2D	Two-dimensional
AFM	Atomic force microscope
DC	Direct current
e-beam	Electron beam
FESEM	Field emission scanning electron microscope
FFT	Fast Fourier transform
FWHM	Full width half-maximum
IR	Infrared
LPCVD	Low-pressure chemical vapor deposition
MBE	Molecular beam epitaxy
MOCVD	Metal-organic chemical vapor deposition
NIR	Near infrared
PAA	Porous anodic alumina
PL	Photoluminescence
PVD	Physical vapor deposition
RF	Radio frequency
UV-Vis	Ultraviolet-visible

KAJIAN SIFAT MORFOLOGI DAN OPTIK KE ATAS ALUMINA ANODIK BERLIANG

ABSTRAK

Alumina anodik berliang (PAA) telah dikajikan dengan luas sejak beberapa dekad yang lalu oleh kerana keberkesanan dan kemudahannya untuk memberikan nanoberliang susunan tersendiri, yang sangat baik sebagai satu templat untuk penciptaan nanostruktur. Untuk memperkenalkan lebih kebolehlaksanaan dalam proses anodik PAA, percubaan untuk menciptakan PAA yang tersusun perlu dilakukan pada suhu bilik tanpa sistem penyejukan. Selain itu, suatu bahan yang kos efektif perlu dikajikan untuk digunakan sebagai elektrod lawan. Dalam projek ini, kerja ditumpukan kepada kajian atas penciptaan dan pencirian PAA di bawah pelbagai pembolehubah anodik, termasuk voltan anodik, jenis substrat aluminium, kepekatan elektrolit dan jenis elektrod lawan. Ia telah ditemui bahawa permukaan aspek morfologi PAA adalah signifikan bergantung kepada pembolehubah anodik yang telah dikajikan. Saiz liang adalah linear bergantung kepada voltan anodik daripada 20 kepada 40 V, berubah dalam julat 30 kepada 50 nm. Walau bagaimanapun pada 50 V, selepas proses meluaskan liang, PAA terpatah menjadi struktur berserabut. Kesan jenis substrak aluminium yang berbeza juga telah ditunjukkan. Aluminium dengan bijirin yang sebesar 283 nm adalah sukar untuk diciptakan menjadi PAA yang seragam walaupun selepas dua langkah proses anodik. Tambahan pula, kehantaran optik menunjukkan nilai yang lebih tinggi dengan pengurangan dalam saiz liang, dan pinggir interferens yang lebih besar dalam kehantaran spektrum menunjukkan permukaan PAA yang lebih licin. Sebagai tambahan, ciri-ciri struktur PAA yang diciptakan

dengan kepekatan asid sulfurik yang berbeza, daripada 1.0 kepada 1.6 M telah dilaporkan. Dengan melakukan analisis kuantitatif pada dua-dimensi (2D) jelmaan Fourier pantas (FFT), 1.4 M telah ditemui sebagai kepekatan asid sulfurik yang optimum untuk menumbuhkan PAA dengan kekerapan yang terbaik. Kebulatan liang kekal pada sekitar 0.87 dan tidak menunjukkan perbezaan yang signifikan dalam julat kepekatan. Sebaliknya, saiz liang dan keliangan PAA meningkat dengan peningkatan kepekatan asid sulfurik, daripada 18.4 kepada 26.7 nm dan 21.0 kepada 33.8%, masing-masing. Satu trend yang serupa oleh nisbah jalur pelepasan fotoluminesen (PL), F/F^+ dan nisbah kekerapan PAA telah ditunjukkan, dan hubungan antara kekerapan susunan liang dengan PL telah dijelaskan selanjutnya. Akhirnya, ciri-ciri struktur PAA yang diciptakan dengan jenis elektrod lawan yang berbeza telah ditentukan. PAA dengan kekerapan yang terbaik adalah ditumbuhkan dengan grafit sebagai elektrod lawan di bawah pembolehubah anodik yang tertentu, berbanding kepada kuprum dan platinum. Lebih-lebih lagi, PAA yang dicipta dengan grafit juga menpunyai kebulatan liang, diameter liang dan keliangan yang tertinggi, iaitu 0.85, 28.5 nm dan 29.8%, masing-masing.

STUDY ON THE MORPHOLOGICAL AND OPTICAL PROPERTIES OF POROUS ANODIC ALUMINA

ABSTRACT

Porous anodic alumina (PAA) has been investigated extensively over the last few decades due to its effectiveness and simplicity to grow self-ordered nanopores, which is excellent as a template for nanostructures fabrication. To introduce more feasibilities in anodizing PAA, the attempt to fabricate highly ordered PAA should be done at room temperature without cooling system. Besides, a more cost effective material should be investigated to be used as a counter electrode. In this project, works are focused on the investigation of fabrication and characterizations of PAA under various anodizing parameters, including anodizing voltage, type of aluminum substrate, concentration of electrolyte and type of counter electrode. It was found that the surface morphological aspects of PAA are significantly dependent on the anodizing parameters that have been investigated. The pore size is linearly dependent on the anodizing voltage from 20 to 40 V, varying in the range of 30 to 50 nm. However at 50 V, after pore widening process, the PAA is fractured into fibrous structure. The effect of different types of aluminum substrates on anodization was also demonstrated. The aluminum with grains as huge as 283 nm is difficult to fabricate into uniform PAA even after two-step anodization. Furthermore, the optical transmittance shows higher value as decreasing in pore size, and the larger interference fringes in transmittance spectra indicate a smoother surface of PAA. In addition, the structural features of PAA fabricated with different sulfuric acid concentrations, from 1.0 to 1.6 M were reported.

By performing quantitative analysis on two-dimensional (2D) fast Fourier transform (FFT), 1.4 M was found to be the optimum concentration of sulfuric acid to grow PAA with best regularity. The pore circularity remains at around 0.87 and shows no significant difference within the concentration range. On the other hand, pore size and porosity of PAA increased with the increasing concentration, from 18.4 to 26.7 nm and 21.0 to 33.8%, respectively. A similar trend of photoluminescence (PL) emission bands ratio, F/F^{+} and the regularity ratio of PAA was shown, and the relationship between pore arrangement regularity and PL was further explained. Finally, the structural features of PAA fabricated with different types of counter electrodes were determined. PAA with the best regularity is grown with graphite as counter electrode under specific anodizing conditions, compared to copper and platinum. Moreover, PAA fabricated with graphite also appeared to have the highest pore circularity, pore diameter and porosity of 0.85, 28.5 nm and 29.8%, respectively.

CHAPTER 1

INTRODUCTION

1.1 Nanotechnology and Nanostructures

Nanotechnology is the study of functional systems at atomic or molecular scale. Generally, nanotechnology includes the development of materials that have dimensions at the scale between 1 and 100 nm. Applications of these materials have already been introduced and expected to have great potential in all scientific fields, like optoelectronics, renewable energy, chemical catalysis, medical devices and biomedicine. The materials at nanoscale have a relatively larger surface area to volume ratio compared with the same materials at larger scale, which makes them have stronger surface effects. Besides, quantum effects begin to dominate the behavior of matter at nanoscale and will significantly change the electrical, magnetic and optical properties of the materials.

Similar as nanotechnology, nanostructures refer to material systems with length scale in the range of 1 to 100 nm in at least one dimension. Out of these structures, one-dimensional (1D) nanostructures, such as nanowires and nanorods are of great interest due to their potential implications and feasibility of applications in semiconductors and nanoelectronics. 1D nanostructures enable efficient transport of electrons, as well as exhibit the unique quantum confinement effect, which is important for the applications. The amount of energy required to confine excitation levels in nanostructures is increased because the size of the structure is actually smaller than the wavelength of light emitted (Cong et al., 2002). By controlling the diameter, growth orientation, length, and crystallinity of the nanowires and nanorods, it is possible to

control the wavelength of energy and consequently control the physical, electrical, magnetic and optical properties.

By having uniform channels of nanometer dimension, nanochannel-array materials have attracted considerable interest in recent years as they can be employed as templates used for manufacturing 1D nanostructures. To fabricate nanoporous membranes with ordered pore arrangements, lithography patterning is one of the common techniques that has been introduced which offer ultra-high precision. However, even with advanced lithographic techniques such as electron beam (e-beam) and X-ray lithographies, certain major drawbacks exist. A low aspect ratio of the formed nanoporous limit the applications of lithography techniques, not to mention it required sophisticated facilities and high preparation cost. Highly ordered nanoporous metal oxide structures including alumina and titania have been successfully fabricated by electrochemical anodization of metals (Masuda and Fukuda, 1995; Sulka et al., 2010). The economic feasibility and technologic consistency of this method have solved most of the drawbacks of lithography-based techniques.

1.2 Anodization of Aluminum

Anodization (anodic-oxidation) is an electrochemical process carried out by applying positive voltage to anode in an electrolyte to increase the oxide layer thickness of the anode. When aluminum is employed as anode, by anodizing it is able to produce two types of oxide layer: barrier oxide layer and porous oxide layer. The main factor to determine the oxide layer type grown on the aluminum is the electrolyte used during the anodizing process (Keller et al., 1953). The barrier oxide layer can be formed by anodizing in weak acid or neutral solution (pH = 5 – 7), such as boric acid, ammonium borate, ammonium tartrate and aqueous phosphate solutions. In contrast,

porous oxide layer can be formed by anodizing in stronger acidic electrolytes, includes sulfuric, oxalic, phosphoric and chromic acid (Keller et al., 1953; O'Sullivan and Wood, 1970).

The porous oxide layer obtained in this manner is also called porous anodic alumina (PAA). PAA has been investigated extensively over the last few decades due to its effectiveness and simplicity to grow self-ordering nanopores, which is a suitable template for nanostructure fabrication. The hexagonally closed packed structure of PAA was first reported by Keller et al. in 1953 (Keller et al., 1953). In 1995, Masuda and Fukuda developed a two-step replicating process to achieve a uniform honeycomb structure PAA (Masuda and Fukuda, 1995). Recently, anodization of aluminum has become one of the most common methods for the synthesis of highly ordered nanostructures.

1.3 Problem Statement

Majority of the studies show that in order to obtain highly ordered PAA, anodization under low temperature around 1 to 10 °C is required. Besides, platinum is always the primary choice as counter electrode in the anodizing system because it is inert to almost all of the chemical reactions and conducting electricity well. The dependent on cooling system to allow aluminum anodized under low temperature as well as expensive platinum counter electrode have increased the cost of the process. To introduce more feasibility in anodizing PAA, the attempt to fabricate highly ordered PAA should be done at room temperature. An alternative counter electrode should be discovered as well to reduce the cost of anodization.

porous oxide layer can be formed by anodizing in stronger acidic electrolytes, includes sulfuric, oxalic, phosphoric and chromic acid (Keller et al., 1953; O'Sullivan and Wood, 1970).

The porous oxide layer obtained in this manner is also called porous anodic alumina (PAA). PAA has been investigated extensively over the last few decades due to its effectiveness and simplicity to grow self-ordering nanopores, which is a suitable template for nanostructure fabrication. The hexagonally closed packed structure of PAA was first reported by Keller et al. in 1953 (Keller et al., 1953). In 1995, Masuda and Fukuda developed a two-step replicating process to achieve a uniform honeycomb structure PAA (Masuda and Fukuda, 1995). Recently, anodization of aluminum has become one of the most common methods for the synthesis of highly ordered nanostructures.

1.3 Problem Statement

Majority of the studies show that in order to obtain highly ordered PAA, anodization under low temperature around 1 to 10 °C is required. Besides, platinum is always the primary choice as counter electrode in the anodizing system because it is inert to almost all of the chemical reactions and conducting electricity well. The dependent on cooling system to allow aluminum anodized under low temperature as well as expensive platinum counter electrode have increased the cost of the process. To introduce more feasibility in anodizing PAA, the attempt to fabricate highly ordered PAA should be done at room temperature. An alternative counter electrode should be discovered as well to reduce the cost of anodization.

1.4 Research Objectives

The objectives of this project are:-

1. To investigate the morphological and optical properties of PAA for various anodizing parameters at room temperature, i.e. anodizing voltage, substrate condition, acid concentration and type of counter electrode.
2. To improve the simplicity of the formation of PAA without using cooling system during anodizing process while maintaining the control of PAA structures.
3. To examine the formation of PAA with two different aluminum deposition methods, i.e. direct current (DC) sputtering and electron-beam (e-beam) evaporation on glass substrate which could be useful for optical applications.
4. To have quantitative study on the morphological properties of PAA with two-dimensional (2D) fast Fourier transform (FFT).
5. To explore the alternative for platinum as counter electrode in fabricating PAA.

1.5 Originality of Research

The original work of this research project is the investigation of optical properties including transmittance and photoluminescence of PAA. Unlike structural properties, the optical properties of PAA are scarcely studied and still not well documented. Besides, the quantitative study done on morphological properties of PAA especially pore arrangement regularity by using 2D FFT is a new yet reliable method. Apart from that, the study of the effect of counter electrode on PAA was performed and this work has not been reported in the literature. Finally, highly ordered PAA were

successfully grown at room temperature, which usually only been synthesized at low temperature.

1.6 Outline of Thesis

Chapter 2 encompasses a literature review of PAA, including the overview of alumina, growth mechanism, factors influencing the morphological and optical properties of PAA. Some applications of PAA are also included.

Chapter 3 describes the experimental setup and growth conditions. Besides, the principle operation of instrumentations that involved in this project are also covered.

Chapter 4 presents the characterization results of the synthesized PAA under various anodizing parameters, including anodizing voltage, type of aluminum substrate, concentration of electrolyte and type of counter electrode. Analysis and discussion are also done in the same chapter.

Chapter 5 summarizes the project as a conclusion and the possible future work that can be done.

CHAPTER 2

LITERATURE REVIEW

2.1 Introduction

In this chapter, a brief overview of PAA is presented. The review includes the growth mechanism of pores on PAA and the factors that will influence the morphological and optical properties of PAA.

2.2 Overview of Alumina

Alumina, also known as aluminum oxide or specifically aluminum(III) oxide is the chemical compound of aluminum and oxygen with chemical formula of Al_2O_3. It can exist in several crystalline phases, such as cubic γ phase and η phase, monoclinic θ phase, hexagonal χ phase, orthorhombic κ phase and tetragonal or orthorhombic δ phase, which all revert to the most stable hexagonal α phase known as corundum at elevated temperatures (Levin and Brandon, 1998; Paglia, 2004). Figure 2.1 shows the hexagonal structure of α-alumina.

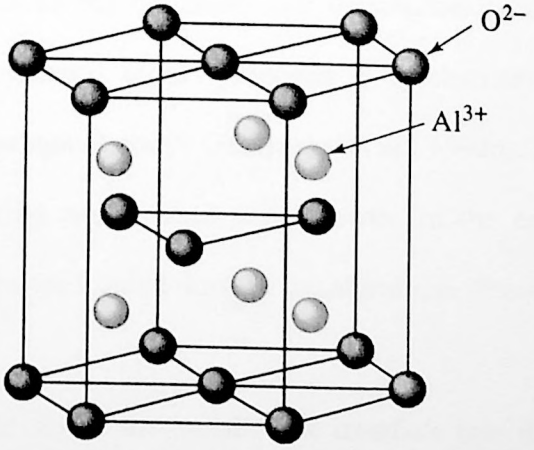

Figure 2.1: Hexagonal structure of α-alumina (Perez, 1997).

However, it should be noted that the alumina formed by anodization is amorphous. Alumina is one of the most cost efficient and commonly used material in the engineering ceramics field. It is an electrical insulator but has a relatively high thermal conductivity for a ceramic material. Besides, it is insoluble in water. Alumina is able to react with both acids and bases by acting as an acid with a base and as a base with an acid, then neutralizing the other and producing salt, showing its amphoteric nature. Table 2.1 shows the basic properties of alumina (99.7% purity) under the temperature of 20 °C.

Table 2.1: Basic properties of alumina under 20 °C (Davis, 2010).

Properties	Values
Density (g cm^{-1})	3.96
Tensile strength (MPa)	220
Melting point (°C)	2072
Boiling point (°C)	2977
Thermal conductivity (W m^{-1} K^{-1})	28
Dielectric constant at 1 MHz	9.7

2.3 Mechanism for Pore Formation

Despite the extensive studies of anodization, the mechanism for pore formation in PAA is still not been fully comprehended. Fundamentally, PAA are believed to form as a result of combination of the oxidation and dissolution of aluminum during anodization. In 1998, Jessensky et al. proposed a mechanism to explain the phenomenon of ordered hexagonal arrays (Jessensky et al., 1998a). Figure 2.2 shows the migration of ions during steady state pore growth. In the early stage of the anodizing process, Al^{3+} ions are formed through the aluminum dissolution reaction:

$$Al \rightarrow Al^{3+} + 3e^{-} \quad (2.1)$$

and migrate from the metal across the metal/oxide interface into the forming oxide layer. Meanwhile O^{2-} and OH^{-} ions present in electrolyte, migrate to the

oxide/aluminum interface. The anions will combine with the Al^{3+} ions and contribute to the oxide formation, which can be expressed as below:

$$2Al^{3+} + 3O^{2-} \rightarrow Al_2O_3 \quad (2.2)$$

$$2Al^{3+} + 3OH^{-} \rightarrow Al_2O_3 + 3H^{+} \quad (2.3)$$

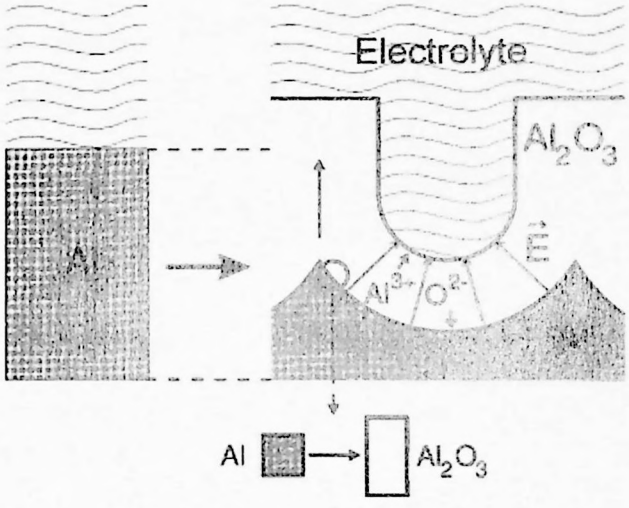

Figure 2.2: Migration of Al^{3+} and O^{2-} ions during steady state anodization. The arrows in alumina indicate migration of ions and direction of oxide layer grow (Jessensky et al., 1998a).

The atomic density of aluminum existing in alumina is lower than the metallic aluminum by a factor of two. The mechanical stress caused by the expansion during oxidation formation at the metal/oxide interface is a possible origin of forces between neighbouring pores. Since the oxidation process takes place at the entire pore bottom simultaneously, the oxide layer can only expand in the vertical direction, hence the existing pore walls are pushed upwards. At steady state, the oxidation and dissolution rates are equal, so the barrier layer does not grow any thicker. Instead, the pores will grow deeper.

The pore formation of PAA is frequently explained with current-time transient plot, as shown in Figure 2.3. During the initial stage of the anodizing process under

constant voltage, the aluminum surface is covered by a uniform and compact oxide layer, which causes the current density to drop rapidly due to high resistance (Stage a). Further anodizing results in nucleation of the pores on the barrier film (Stage b). At the minimum of current density, electric field-assisted dissolution of the oxide layer takes place and the first localized pores are formed and become sites for further pore growth (Stage c). Finally, the steady state growth of porous alumina is reached and the current density is almost constant (Stage d).

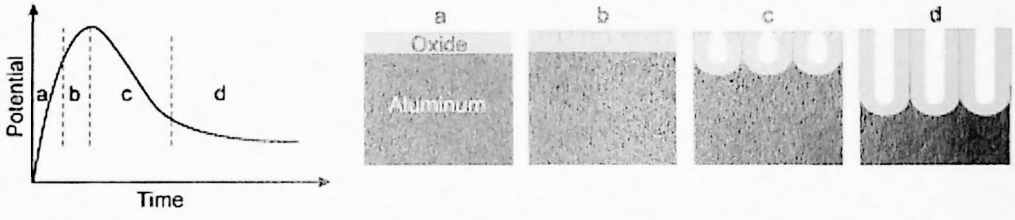

Figure 2.3: Current-time transient plot and schematic diagrams of corresponding stages of PAA development (Sulka, 2008).

2.4 Influence of Anodization Conditions and Treatments on Morphological Properties of PAA

Figure 2.4 illustrates the structure of an ideal PAA. PAA are often characterized by given parameters such as pore diameter, wall thickness, barrier layer thickness and interpore distance (cell diameter). The dependence of the aluminum pre-treatments, the anodizing conditions, as well as the post-treatments on these physical parameters are studied.

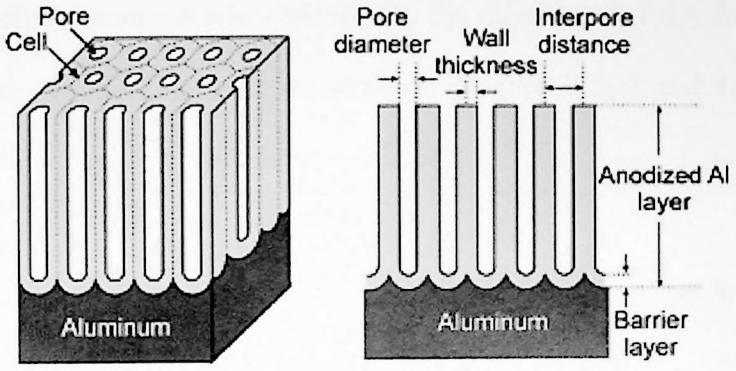

Figure 2.4: Schematic of an ideal PAA (Sulka, 2008).

2.4.1 Pre-treatments

As mentioned previously, pore formation results from two chemical processes: electric field-assisted dissolution of alumina at oxide/electrolyte interface and formation of alumina (oxidation) at the oxide/aluminum interface. The formed alumina will be strongly influenced by the conditions of aluminum substrate. Hence, the treatments on aluminum substrate prior to anodization are important to ensure its physical conditions are utilized for anodizing.

2.4.1.1 Annealing

The annealing of aluminum foil has various advantages. It includes reducing residual stresses and improving the crystallinity of the material (Guo et al., 2011), as well as increases the average size of the grains (Jessensky et al., 1998b). Typically, the temperature of annealing is set at around two-thirds of the melting point of aluminum (400 – 500 °C) for 3 to 5 h under argon or nitrogen ambient. Figure 2.5 shows electron micrographs of PAA with different treatments prior to anodization. The PAA derived from as-rolled aluminum foil given no treatment (Figure 2.5(a)) and oxide heat-treatment (Figure 2.5(b)) appear to have no planar ordering and are of inconstant, noncircular shape. The lines of pores follow the direction of rolling in the aluminum

foil from which the alumina was derived. On the other hand, PAA from aluminum foils that were annealed prior to anodization (Figure 2.5(c) and (d)) was more consistent and the lines of pores were eliminated.

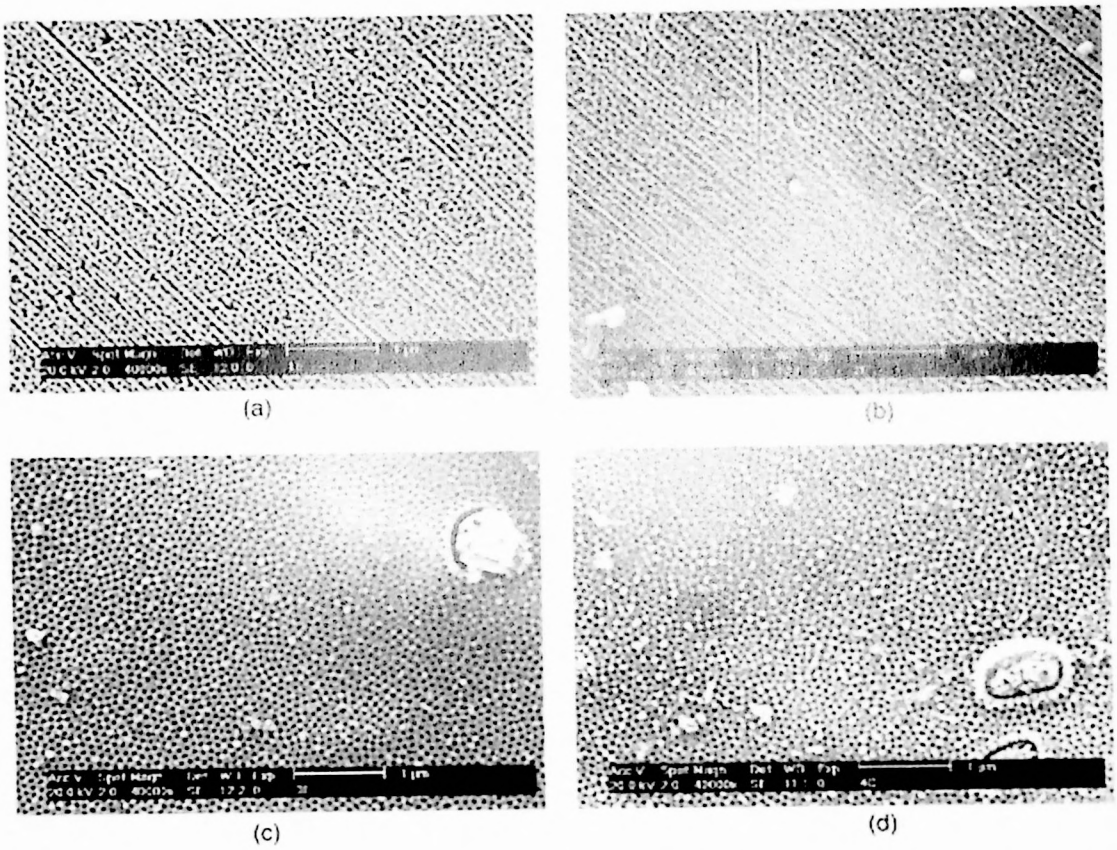

Figure 2.5: Electron micrographs of PAA from anodized in 0.3 M oxalic acid with 4 h second anodization, with (a) no treatments, (b) oxide heat-treatment, (c) foil annealing and (d) foil annealing and oxide heat-treatment (Lo and Budiman, 2007).

2.4.1.2 Polishing

Polishing is a common method used for surface planarization to offer a more flat and smooth surface. This is essential for anodizing because the pore formation process can be made spatially periodic by patterning an extremely smooth aluminum substrate. Polishing can be categorized into a few types: mechanical polishing, chemical polishing and electropolishing. Among of them, electropolishing is the mostly used method. L_1 electrolyte consisting of 62 cm^3 perchloric acid, 700 cm^3

ethanol, 100 cm^3 butyl cellusolve and 138 cm^3 distilled water is a well-known electrolyte that used to electropolish aluminum (Ricker et al., 1996). Figure 2.6 shows patterns that formed on the aluminum film surface by electropolishing with L_1 electrolyte at various voltages and durations. Two distinctly different surface morphologies could be obtained: parallel stripes (50 V, 10 s) and "egg-carton" pattern (60 V, 30 s) which has a hexagonal close-packed arrangement of crests.

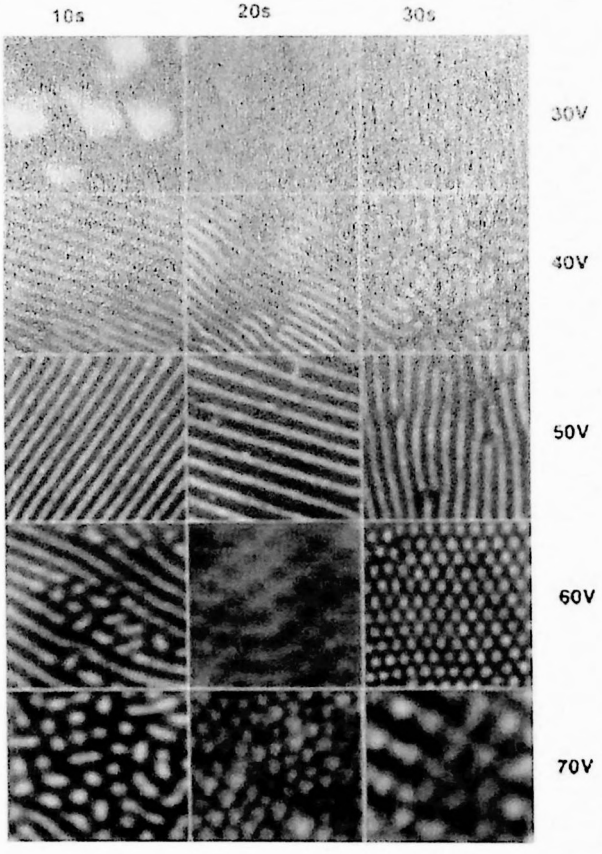

Figure 2.6: AFM images of electropolished aluminum for different conditions at 15 °C. Scan area: 6 × 6 μm (Ricker et al., 1996).

Another commonly used electrolyte for electropolishing aluminum is mixed solution of perchloric acid and ethanol (Zhao et al., 2006). Figure 2.7 shows the atomic force microscope (AFM) images of the aluminum surface after electropolish. Similar

stripes as some of in Figure 2.6 could be observed. These patterns can act as self-assembled masks for nanopores formation during anodization.

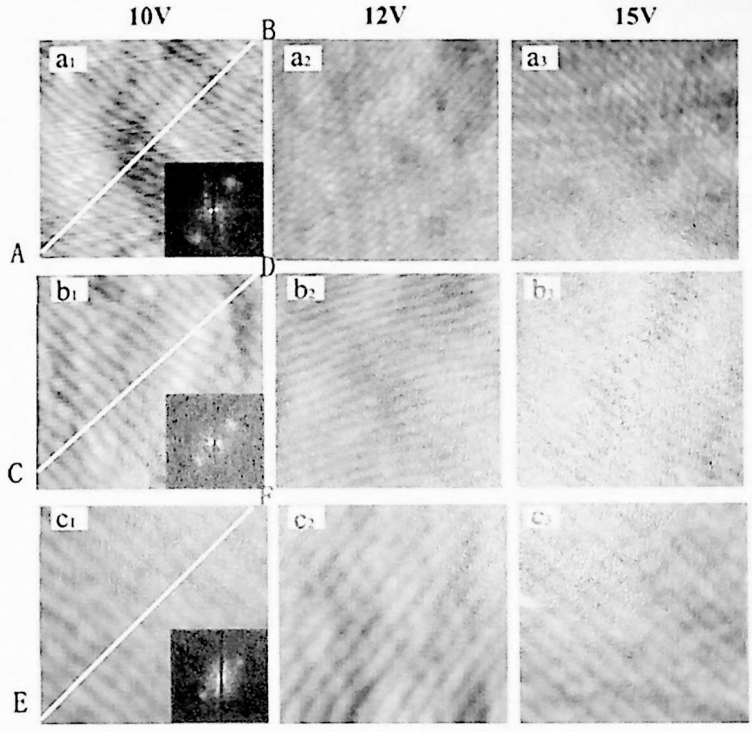

Figure 2.7: AFM images of aluminum surface after electropolish under various voltages for 180 s in perchloric acid-ethanol solution with different volume ratio: (a) 4:6, 2000 × 2000 nm, (b) 3:7, 1000 × 1000 nm and (c) 2:8, 500 × 500 nm. The 2-dimensional fast Fourier transforms of 10 V are shown as inset (Zhao et al., 2006).

2.4.2 Anodizing Conditions

2.4.2.1 Anodizing Type

Several types of anodization have been proposed in the literature. The process of PAA formation at low current density is called mild anodization. This anodizing method is able to obtain highly ordered PAA structures but its shortcoming lies in increased duration of the process. On the other hand, the current density used during hard anodization is much higher than in mild anodization and makes it possible to form highly ordered PAA in much shorter time. However, high field current from hard anodization introduces much evolution of heat. In order to avoid breakdown of the

oxide film during hard anodization, any excessive heat should be removed effectively and the aluminum is usually pre-anodized at a constant current density or constant voltage for few minutes (Sulka, 2008). Table 2.2 shows the different conditions for mild and hard anodization. For each electrolyte, there is a range of anodizing voltage which can be applied without breakdown. From the range, there is an optimum value of the anodizing voltage at which, the best arrangement of nanopores is observed.

Table 2.2: Mild and hard anodizing conditions of PAA (Sulka, 2008).

	Electrolyte concentration (M)	Temperature (°C)	Range of voltage (V)	Optimum voltage (V)	Ref.
Mild	0.3 H_2SO_4	10	10 – 25	25	1,2
	2.4 H_2SO_4	1			3,4
	6.0 H_2SO_4	20		18	5
	0.3 $H_2C_2O_4$	1 – 5	30 – 100	40	2,6
		15 – 20			3,7,8
	0.2 – 0.3 H_3PO_4	0 – 5	160 – 195	195	3,9,10
	H_3PO_4:CH_3OH:H_2O (1:10:89, v/v)	-4			11
Hard	1.8 H_2SO_4	0	40 – 70	70	12
	0.03 – 0.06 $H_2C_2O_4$	3	100 – 160	160	12
	0.3 $H_2C_2O_4$	1	110 – 150	120 – 150	13
	0.1 H_3PO_4	0	195 – 235	235	12
	H_3PO_4:C_2H_5OH:H_2O (1:20:79, v/v)	-10 – 0	195	195	14

1. (Masuda et al., 1997a)
2. (Li et al., 1999)
3. (Ono et al., 2004)
4. (Sulka and Parkoła, 2007)
5. (Masuda et al., 2006)
6. (Shingubara et al., 1997)
7. (Hwang et al., 2002)
8. (Kashi and Ramazani, 2005)
9. (Jessensky et al., 1998b)
10. (Masuda et al., 1998)
11. (Li et al., 2000a)
12. (Chu et al., 2006)
13. (Lee et al., 2006)
14. (Li et al., 2006)

Since two-step anodization been proposed by Masuda and Satoh to form highly ordered PAA (Masuda and Satoh, 1996), one-step anodization is rarely been used due to worse ordered PAA results. After first step anodization, chemical etching of the formed oxide layer is carried out in a mixed solution containing 6 wt.% of phosphoric acid and 1.8 wt.% of chromic acid at a temperature of 60 to 80 °C (Li et al., 1999). The time required for the chemical etching of oxide depends heavily on the first anodization, which must be at least half of the anodization time to ensure an ordered pore structure (Erdogan et al., 2012).

Recently, Chung et al. have demonstrated a new anodizing method known as hybrid pulse anodization, combining pulse reverse (alternate between positive and small negative) and pulse (alternate between positive and zero) voltages as a two-step anodization (Chung et al., 2009). The small negative voltage could overcome the limitation of conventional low temperature anodization to form nanopores in low purity aluminum at room temperature without heat treatment and cooling. Hybrid pulse anodization can enhance distribution uniformity of PAA by minimized the heat fluctuation at room temperature.

2.4.2.2 Types of Electrolyte and Anodizing Voltages

The structural features of PAA depend on the electrolyte and the applied anodizing voltage. The interpore distance of the PAA lattice formed by the self-organized anodization heavily depends on the anodizing voltage. Highly ordered PAA are fabricated by two-step anodizing in sulfuric, oxalic and phosphoric acid solutions under voltages of 25, 40 and 160 V, respectively (Li et al., 1999). Figure 2.8 shows the electron micrographs of the bottom of pores after pores opening. From there, it is

evident that the highest density of nanopores can be obtained by anodizing in sulfuric acid compared to other electrolytes.

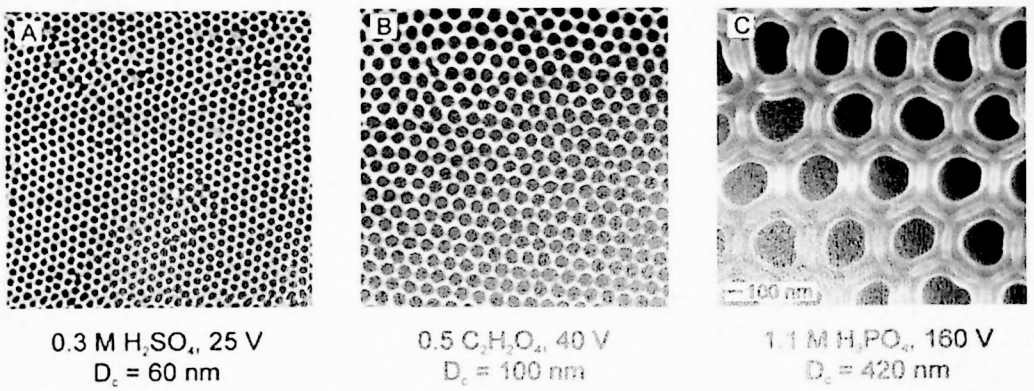

Figure 2.8: Electron micrographs of PAA bottom-views fabricated by different electrolytes after pores opening (Li et al., 1999).

Besides, PAA formed in the same electrolyte, but different anodizing voltages are presented in Figure 2.9, which shows the increasing of interpore distance as the increasing of anodizing voltage. The relationship between anodizing voltages used for anodization and the corresponding interpore cell diameters for various electrolytes are presented in Figure 2.10. It shows linear regardless of the type of electrolyte used, as the equation:

$$D_{int} = \lambda_i \cdot U \tag{2.4}$$

where D_{int} is the interpore distance, λ_i is the proportional constant approximately 2.5 nm V^{-1} and U is the anodizing voltage (Nielsch et al., 2002).

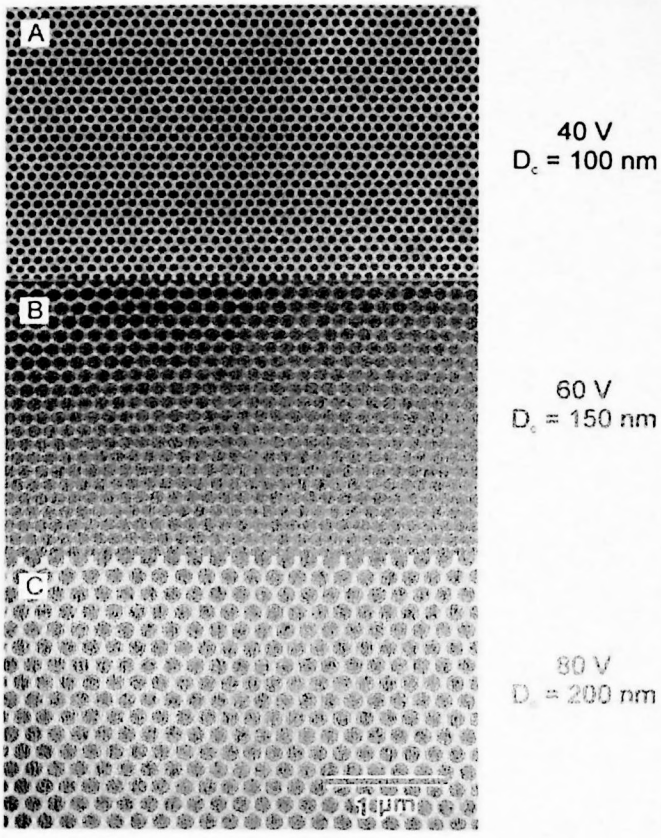

Figure 2.9: Electron micrographs of perfectly ordered PAA formed from pre-textured aluminum at different anodizing voltage in 0.3 M oxalic acid (Masuda et al., 1997b).

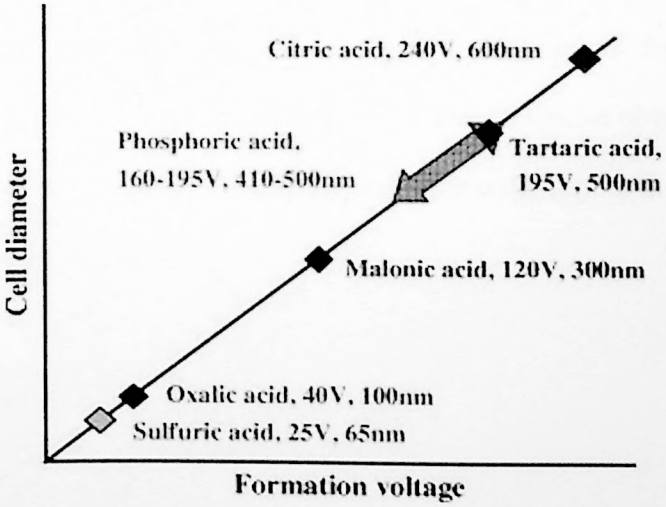

Figure 2.10: Self-ordering voltages and corresponding cell diameters plot (Ono et al., 2005).

From literature, the pore diameter is also linearly proportional to the anodizing voltage, with lower proportional constant approximately 1.29 nm V^{-1} (O'Sullivan and Wood, 1970), indicating the dependence of the pore diameter on anodizing voltage is less sensitive than interpore distance. For the case of porosity, two different behaviors have been observed. At low temperature of -8 and 1 °C, the porosity of PAA decreases as the anodizing voltage increases. On the other hand, increasing anodizing voltage increases the porosity of PAA formed under 10 °C (Sulka and Parkoła, 2007). However, according to Nielsch et al., the optimum porosity of self-ordering PAA should be 10% regardless of anodizing conditions (Nielsch et al., 2002).

2.4.2.3 Electrolyte Temperature

The effect of electrolyte temperature on pore diameter, interpore distance and porosity of PAA was studied by Sulka and Parkoła (Sulka and Parkoła, 2007). The pore diameter and interpore distance increase linearly with increasing anodizing voltage, which is in a good agreement with previous section. The interpore distance does not vary significantly with the temperature of anodization. By increasing the temperature of the electrolyte, an increase in pore diameter can be observed. However, as shown in Figure 2.11, the pore is not circular and the order is poor at 10 °C compared to the lower temperatures.

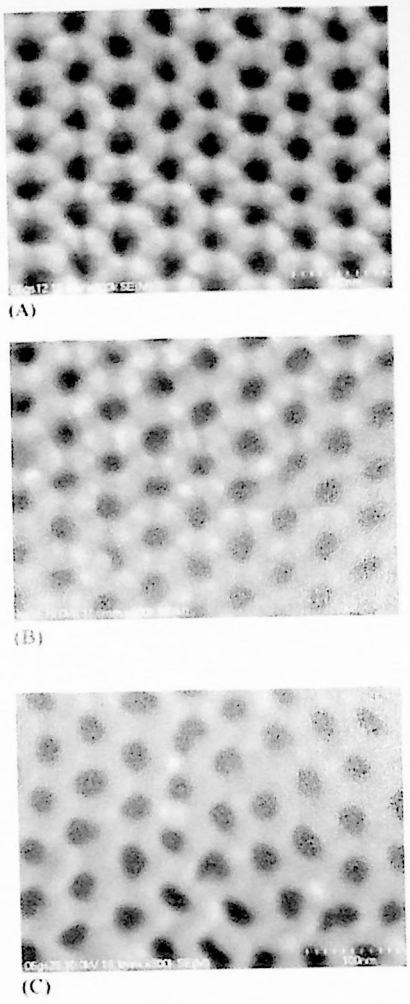

Figure 2.11: Electron micrographs of PAA formed at various temperatures: (A) -8 °C, (B) 1 °C and (C) 10 °C (Sulka and Parkoła, 2007).

2.4.2.4 Anodizing Duration

With increasing anodizing duration, an increase in pore diameter could be observed. The pore diameter increase with anodizing time due not only to the chemical dissolution of oxide but also the coalescence and formation of stable pore walls (Choo and Devereux, 1975). For two-step anodization, the anodizing duration for first step can effectively improves the regularity of final PAA produced (Turkevych et al., 2012).

Selected anodizing conditions and the respective structural features are collected and presented in Table 2.3.

Table 2.3: Structural features of nanostructures obtained by anodizing at various anodizing conditions (Sulka, 2008).

Acid	Concentration (M)	Temperature (C)	Voltage (V)	Pore diameter (nm)	Interpore distance (nm)	Porosity (%)	Pore density (cm^{-2})	Anodizing step	Ref.
Sulfuric acid	0.18	10	25	24	66.3	12.0	2.63×10^{10}	2-step	1,2
	0.3	10	25	-	60	-	3.2×10^{10}	1-step	3
	1.1	5	25	36	64	28.7	2.8×10^{10}	2-step	4
	1.7	-	10 – 15	10 – 20	-	-	-	1-step	5
	1.8	0.1 – 5	15 – 25	10 – 20	44.8 – 65.0	4.5 – 8.6	$5.8 – 2.7 \times 10^{10}$	1-step	6
	1.8	0.1	40 – 70 [a]	30 – 50	90 – 130	10.0 – 13.5	$1.4 – 0.7 \times 10^{10}$	1-step	6,7
	2.4	-8 – 10	15 – 25	13.4 – 27.0	39.7 – 68.7	10.3 – 20.5	$7.3 – 2.4 \times 10^{10}$	2-step	8
	6.0 – 8.0	0 or 20	18	30	45	40.3	5.7×10^{10}	2-step	9
Oxalic acid	0.03 – 0.06	3	100 – 160 [a]	50 – 100	220 – 440	4.7	$0.24 – 0.06 \times 10^{10}$	1-step	7
	0.15	-1	70	90.4	-	26.9	0.42×10^{10}	1-step	10,11
		16		87.4		21.9	0.36×10^{10}		
	0.15	5	10 – 60	11 – 39	40.6 – 141	6.6 – 6.9	$7.0 – 0.6 \times 10^{10}$	2-step	12
	0.3	1	110 – 150 [a]	49 – 59	220 – 300	3.3 – 3.5	$1.3 – 1.9 \times 10^{10}$	2-step	13
	0.3	1	40	31	105	8.0	1.05×10^{10}	2-step	1,2
	0.3	15	20 – 60	-	49.8 – 159.8	-	$4.6 – 0.45 \times 10^{10}$	2-step	14
			40	24	109	4.4	0.97×10^{10}		
	0.45	5	40 – 50	36 – 57	105 – 114	10.7 – 22.7	$1.05 – 0.89 \times 10^{10}$	2-step	4
Phosphoric acid	0.04 – 0.4	-1 – 16	160	170 – 200	-	14.0 – 26.0	5.0×10^{12}	1-step	11
	0.1 – 0.25	0	195 – 235 [a]	130 – n.a.	420 – 480	8.7 – n.a.	$6.5 – \text{n.a.} \times 10^{8}$	1-step	7
	0.1	3	195	158.4	501	9.0	4.6×10^{8}	1-step	1,2
	0.3 – 1.1	0	195	-	500	-	4.6×10^{8}	1-step	15
	0.53	n.a.	40 – 120	60 – 200	n.a.	n.a.	n.a.	1-step	5
	1.1	3	160	n.a.	420	n.a.	6.5×10^{8}	1-step	3

Table 2.3 continued

[a] = hard anodization
1. (Nielsch et al., 2002)
2. (Li et al., 1999)
3. (Li et al., 1998)
4. (Schneider et al., 2005)
5. (Sadasivan et al., 2005)
6. (Chu et al., 2005)
7. (Chu et al., 2006)
8. (Sulka and Parkoła, 2007)
9. (Masuda et al., 2006)
10. (Bocchetta et al., 2002)
11. (Bocchetta et al., 2003)
12. (Shingubara et al., 1997)
13. (Lee et al., 2006)
14. (Hwang et al., 2002)
15. (Masuda et al., 1998)

2.4.3 Post-Treatments

The main application of PAA is to be used as templates for other nanomaterials fabrication. Hence, the films are always subjected to further post-treatment processes such as removal of aluminum and barrier layer in order to improve its viability as a template.

2.4.3.1 Removal of Aluminum

The most common method to remove aluminum substrate is chemical etching by immersing the sample in a saturated $HgCl_2$ solution for few hours (Jia et al., 2006). There are also another solutions such as $CuCl_2$/HCl (Chen et al., 2005) and $CuSO_4$/HCl (Ding et al., 2005) that are used for aluminum removal by different groups to avoid highly toxic mercury. It was found that the duration needed for effective dissolution of a 0.2 mm aluminum is less than 2 min with HCl concentration from 25 to 65% (Ding et al., 2005). Besides, the temperature of solution has a negligible effect on the time of removal.

2.4.3.2 Removal of Barrier Layer

After the PAA film is separated from the aluminum substrate, pore opening is usually carried out in order to make the film through-hole. The removal of barrier layer can be done by chemical etching with phosphoric acid. When the etching time is prolonged, the pores can be widened, which is the pore widening process (Li et al., 2000a). The widened pore diameter can be adjusted by changing the chemical etching time in phosphoric acid, as shown in Figure 2.12.

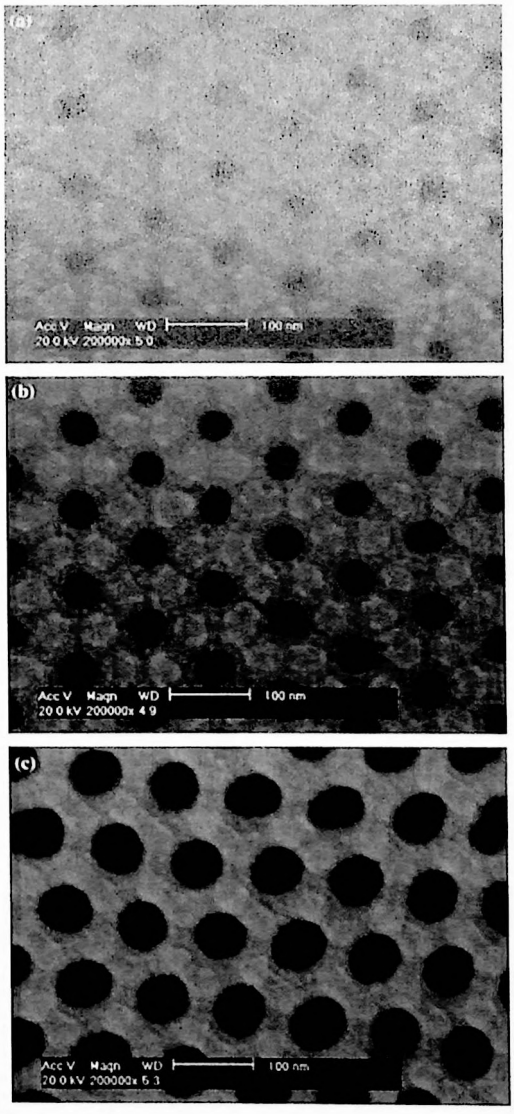

Figure 2.12: Electron micrographs of PAA with etching time of (a) 0 min, (b) 30 min and (c) 50 min (Choi et al., 2006).

A progressive reduction of the anodizing voltage would result in a barrier layer thinning was suggested, due to field-assisted dissolution of oxide (Wood et al., 1968). Zhao et al. have demonstrated an alternative way to remove PAA barrier layer without removing the aluminum substrate in advance by combining the progressive voltage drop and cathodic polarization (Zhao et al., 2007). The second step anodizing voltage was dropped stepwisely and maintained before turned off the voltage supply. Subsequently, cathodic polarization was performed in 0.5 M KCl solution with the PAA/aluminum as cathode and graphite plate as anode under -4 to -5 V.

2.5 Optical Properties of Porous Anodic Alumina

For the application as an optical material, investigation on the optical properties of PAA is essential. The transmittance of PAA on glass substrate were studied by several groups (Chu et al., 2002; Leung et al., 2012; Guo et al., 2011; Yang et al., 2007). Besides, a strong and broad photoluminescence (PL) band was firstly observed in PAA membranes anodized in oxalic acid (Du et al., 1999). Table 2.4 shows a summary of the PL emission bands of as-prepared PAA fabricated under different anodizing conditions from the literature.

Table 2.4: PL emission bands of as-prepared PAA obtained from different conditions of anodization in the literature.

Electrolyte	Concentration (M)	Voltage (V)	Duration		Excitation source, wavelength (nm)	Position of PL peak (nm)	Ref.
			Step 1	Step 2			
Oxalic acid	0.3	40	6 h	10 h	Xe lamp, 348	~445	(Sun et al., 2006)
	0.3	40	10 h	5 – 10 h	Xe lamp, 360	~450	(Du et al., 1999)
	0.5, 0.23, 0.1	40	2 h	24 h	Xe lamp, 280	~405, ~455	(Huang et al., 2003)
	0.3	40	-	-	Xe lamp, 350	470	(Gao et al., 2003)
	0.25	40	Several h	8-20 h	Xe lamp, 265-380	420-465, 460	(Li et al., 2003)
	0.5	20 – 60	1 h	2 h	Xe lamp, 300	409-432, 460-492	(Huang et al., 2005)
	0.3	40	1 h	10 – 60 min	Xe lamp	443, 470	(Chen et al., 2006)
	0.3	40	10 h	4 h	Xe lamp, 350	434, 460	(Liu et al., 2009)
	0.1 – 0.5	5 mA/cm^2 [a]	10 min	22 min	He-Cd laser, 325	~2.6 eV, ~2.9 eV	(Nee et al., 2009)
	0.3	40-70	3-12 h	Several h	Xe lamp, 375	~450, ~500	(Rauf et al., 2010)
	0.3	40	20 min	-	330	425, 478	(Vrublevsky et al., 2011)
Sulfuric acid	0.3	27	10 h	5-10 h	Xe lamp, 360	No obvious peak	(Du et al., 1999)
	0.3	25	-	-	Xe lamp, -	No obvious peak	(Gao et al., 2003)
	0.3	15-27	Several h	8-20 h	Xe lamp, 265-380	365-460, 460	(Li et al., 2003)
	15 wt.%	20	-	-	Xe lamp, 240	295, 340, 395	(Wu et al., 2001)
	0.3	25	3 h	2 h	He-Cd laser, 325	403	(Huang et al., 2006)
	66.7%	200 mA [a]	25 min	-	Xe lamp, 300-380	460, 500-525	(Ghrib et al., 2012)
Phosphoric acid	0.87	40	2 h	24 h	Xe lamp, 280	No obvious peak	(Huang et al., 2003)
Oxalic : Sulfuric = 1 : 1	0.3 : 0.3	25	-	-	Xe lamp, 250	350	(Gao et al., 2003)

[a] Anodization was carried out under constant current (density).